

SiliconPV 2012, 03-05 April 2012, Leuven, Belgium

Impact of the Deposition and Annealing Temperature on the Silicon Surface Passivation of ALD Al₂O₃ Films

S. Bordihn^{a,b*}, I. Kiesow^a, V. Mertens^a, P. Engelhart^a, J.W. Müller^a,
W.M.M. Kessels^b

^a*Q.Cells SE, Sonnenallee 17-21, 06766 Bitterfeld-Wolfen, Germany*

^b*Department of Applied Physics, Eindhoven University of Technology, P.O. Box 513, 5600 Eindhoven, The Netherlands*

Abstract

The effect of the deposition and annealing temperature on the surface passivation of atomic layer deposited Al₂O₃ films was investigated on *n*-type Cz silicon wafers. The deposition temperature was varied between 200 and 500°C and the annealing temperature between 300 and 450°C, respectively. Films prepared at 200 and 300°C showed an improvement of surface passivation with increasing anneal temperature. The Al₂O₃ films grown at 400 and 500°C did not improve by annealing. By corona charging experiments it was revealed that the improvement in surface passivation with increasing anneal temperature of films grown at 300°C can be attributed to a significant increase in chemical passivation with a minor increase in field-effect passivation. For Cz and FZ wafers an identical surface passivation was achieved with the chemical passivation being lower for Cz wafers due to the surface morphology and the field-effect passivation being quite similar. Consequently the field-effect passivation was found to be the more important passivation mechanism.

© 2012 Published by Elsevier Ltd. Selection and peer-review under responsibility of the scientific committee of the SiliconPV 2012 conference. Open access under [CC BY-NC-ND license](https://creativecommons.org/licenses/by-nc-nd/4.0/).

Keywords: Surface passivation; ALD Al₂O₃; Deposition and anneal temperature

1. Introduction

Passivation of Si surfaces is a key step to improve the efficiency of solar cells as discussed in the review article by Glunz [1]. The chemical passivation of Si surfaces is realized by hydrogen bonding to Si dangling bonds that leads to their elimination as defect states [2]. Dielectric thin films are commonly

*Corresponding author. Tel.: +49 (3494) 6699 - 52118
E-mail address: st.bordihn@q-cells.com

employed to provide hydrogen to the surface, in some cases in combination with a forming gas or other anneal steps. High levels of surface passivation have been reported for dielectric films such as single-layer α -SiN_x:H [3, 4], SiO₂ [5] or Al₂O₃ [6] films as well as stacks containing these films, e.g. SiO₂/ α -SiN_x:H, [7-11] SiO₂/Al₂O₃ [12-15] and Al₂O₃/ α -SiN_x:H [16-19]. In recent years especially the interest in atomic layer deposited (ALD) Al₂O₃ films has increased due to their excellent chemical and field-effect passivation [20, 21]. For ALD Al₂O₃ both the deposition temperature [22, 23] and the temperature of the post-deposition annealing step [24] are known to have a significant impact on the presence of hydrogen in the films and at the Si interface and consequently on the chemical passivation induced by the films.

In this work we investigated the effect of the ALD temperature on the properties and growth characteristics of the Al₂O₃ films. Furthermore their effect on the surface passivation of the Al₂O₃ films was evaluated and the role of hydrogen in terms of chemical passivation was addressed. Finally corona charging experiments were performed to distinguish between chemical and field-effect passivation.

2. Experimental

In this study *n*-type Czochralski (Cz) grown Si substrates with a resistivity of 2-3 Ω -cm were used. The wafers were cleaned in a KOH based wet chemical solution to remove the saw damage. Afterwards the wafers received a standard RCA cleaning procedure prior to the ALD of Al₂O₃ films. The thermal ALD process consisted of 330 cycles with Al(CH₃)₃ and O₃ as reactants. The deposition temperature $T_{\text{Deposition}}$ was varied between 200 and 500°C in steps of 100°C. After film deposition the resulting symmetrically passivated lifetime samples were exposed to an annealing step at temperatures T_{Anneal} between 300 and 450°C for 10 min in a N₂ atmosphere.

The surface passivation was expressed in terms of the effective surface recombination velocity S_{eff} . The S_{eff} -values were extracted from the injection dependent effective minority carrier lifetime $\tau_{\text{eff}}(\Delta n)$ that was obtained from photoconductance decay measurements. These measurements were done with a Sinton WCT-120 lifetime tester. The value of S_{eff} is given for an injection level of $\Delta n = 10^{14}$ cm⁻³ taking into account the wafer thickness of 180 μ m and assuming an infinite bulk lifetime. The S_{eff} -values were therefore evaluated as an upper limit, i.e. $S_{\text{eff,max}}$.

By spectroscopic ellipsometry (SE) measurements that were applied after deposition, the film thickness d , growth per cycle (GPC), and film non-uniformity were investigated to verify whether ALD-like process conditions were present during the film growth. The film thickness non-uniformity was calculated by the relation of $(d_{\text{max}} - d_{\text{min}})/(2 \cdot d_{\text{average}})$ [25]. For SE analysis float zone (FZ) *n*-type Si substrates with shiny etched surfaces were used and prepared identical to the Cz substrates. The film non-uniformity was analyzed based on 137 measurement points equally distributed over the wafer area of 149.3 cm².

3. Results and Discussion

The Al₂O₃ film thickness was found to be 30 nm at a deposition at 200°C and decreased to about 20 nm at 500°C. Consequently the GPC decreased with increasing $T_{\text{Deposition}}$ from 0.92 Å/cycle at 200°C to 0.62 Å/cycle at 500°C, as shown in Table 1. The reduced growth per cycle at higher substrate temperatures can be attributed to a loss of reactive surface groups, in particular surface hydroxyl groups, with higher temperatures [26]. The film uniformity is not significantly affected by an increase in $T_{\text{Deposition}}$ and a maximum non-uniformity of $\pm 5\%$ in film thickness was obtained. Considering the fact that the Al(CH₃)₃ precursor has an onset temperature for thermal decomposition of about 330°C [23] it is remarkable that Al₂O₃ films can be synthesized under ALD-like conditions up to a substrate temperature of about 500°C. However we cannot exclude that thermal decomposition partly took place at 500°C.

Table 1. Film thicknesses, growth per cycle and film non-uniformity of ALD Al_2O_3 films as determined from spectroscopic ellipsometry (SE) measurements. The ALD process consisted of 330 cycles

ALD temperature ($^{\circ}\text{C}$)	200	300	400	500
Growth per cycle ($\text{\AA}/\text{cycle}$)	0.92	0.84	0.79	0.62
Film thickness (nm)	30.4	27.7	26.1	20.5
Film non-uniformity (%)		± 5	± 2	± 3

The surface passivation characteristics of the Al_2O_3 films are shown in Fig. 1. In Fig. 1-a $S_{\text{eff,max}}$ is plotted versus $T_{\text{Deposition}}$ and in Fig. 1-b $S_{\text{eff,max}}$ is plotted versus T_{Anneal} . With increasing $T_{\text{Deposition}}$ an increase in $S_{\text{eff,max}}$ was observed independently of T_{Anneal} . The lowest $S_{\text{eff,max}}$ -values were obtained for Al_2O_3 films synthesized at 200 and 300 $^{\circ}\text{C}$ and annealed at 450 $^{\circ}\text{C}$. For these films the $S_{\text{eff,max}}$ -values decreased with increasing T_{Anneal} from 23 cm/s to 4 cm/s and from 93 cm/s to 5 cm/s when the film growth took place at 200 and 300 $^{\circ}\text{C}$, respectively (see Fig. 1-b). Recently the same trend was reported for O_2 -plasma and H_2O -based ALD Al_2O_3 films grown at 200 $^{\circ}\text{C}$ [23, 24]. In this work the highest $S_{\text{eff,max}}$ -values were obtained for Al_2O_3 films grown at 400 $^{\circ}\text{C}$. When these films were annealed at 350 and 400 $^{\circ}\text{C}$ an increase in $S_{\text{eff,max}}$ was observed compared to an anneal at 300 $^{\circ}\text{C}$. When T_{Anneal} was further increased to 450 $^{\circ}\text{C}$ the $S_{\text{eff,max}}$ was reduced to 92 cm/s. Al_2O_3 films synthesized at $T_{\text{Deposition}} = 500^{\circ}\text{C}$ resulted in a quite constant level of $S_{\text{eff,max}} = 130 \pm 30$ cm/s.

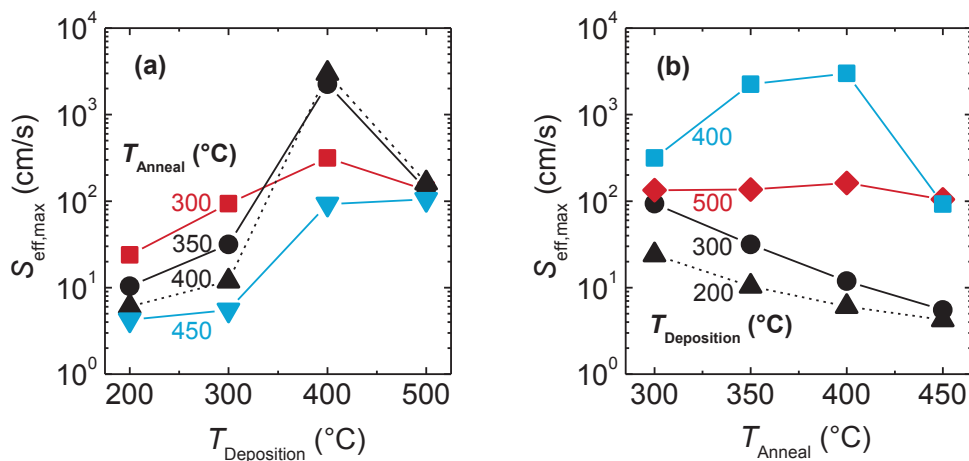


Fig. 1. Effective surface recombination velocity $S_{\text{eff,max}}$ of ALD Al_2O_3 films as a function of (a) deposition temperature $T_{\text{Deposition}}$ and (b) temperature of anneal step T_{Anneal} . The anneal steps were done for 10 min in N_2 ambient

To investigate the origin of the decrease of $S_{\text{eff,max}}$ with increasing T_{Anneal} corona charging experiments were carried out on films grown at 300 $^{\circ}\text{C}$. The technique of corona charging allows for distinguishing between chemical and field-effect passivation [27]. Corona charges were deposited on top of the Al_2O_3 coated substrates and subsequently the $S_{\text{eff,max}}$ and the corona charge density Q_C were measured. This procedure was repeated several times to stepwise increase the total Q_C . That finally results in a plot of $S_{\text{eff,max}}$ versus Q_C . In such a plot the chemical passivation is reflected by the peak height and the shape of the $S_{\text{eff,max}}(Q_C)$ -plot. The field-effect passivation is indicated by the position of Q_C resulting in a maximum value of $S_{\text{eff,max}}$.

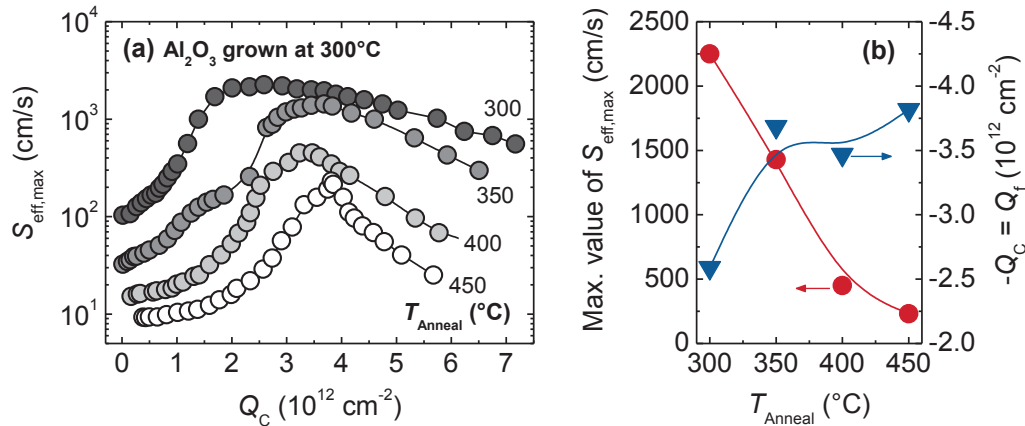


Fig. 2. Effective surface recombination velocity $S_{\text{eff,max}}$ as a function of corona charge density Q_C for Al_2O_3 films synthesized by ALD (330 cycles) at 300°C and annealed for 10 min in N_2 atmosphere. (a) $S_{\text{eff,max}}(Q_C)$ -plots obtained after annealing at temperatures indicated; (b) Related maximum $S_{\text{eff,max}}$ -values and Q_f -values extracted from (a)

At this point the field-effect passivation is nullified and the magnitude of fixed charge density Q_f is about equal to the corona charge density, i.e. $Q_f = -Q_C$. To obtain the $S_{\text{eff,max}}(Q_C)$ -plots for Al_2O_3 films positive charges have to be deposited to nullify the effect of the incorporated negative fixed charge density. The $S_{\text{eff,max}}(Q_C)$ -plots of Al_2O_3 films grown at 300°C and exposed to various anneal steps are shown in Fig. 2-a. The negative Q_f increased slightly from $2 \cdot 10^{12} \text{ cm}^{-2}$ to $4 \cdot 10^{12} \text{ cm}^{-2}$ for samples annealed at 300°C and 450°C , respectively. Therefore higher anneal temperatures slightly improved the level of field-effect passivation. Concerning the chemical passivation, the maximum value of the $S_{\text{eff,max}}(Q_C)$ -plots decreased with increasing T_{Anneal} . After annealing at 300°C maximum values of $S_{\text{eff,max}}$ of 2250 cm/s were obtained whereas after an anneal step at 450°C a value of about ten times lower (230 cm/s) was achieved. In addition it was observed that the peak shape became narrower when T_{Anneal} increased. The change of the maximum value of $S_{\text{eff,max}}(Q_C)$ -plots is shown as function of T_{Anneal} in Fig. 2-b. The $S_{\text{eff,max}}$ dependence on T_{Anneal} for films deposited at 300°C could therefore be related to a significant change in chemical and a minor change in field-effect passivation.

The surface passivation of the Cz Si substrates was compared to FZ wafers that were coated with Al_2O_3 films with identical properties and prepared under the same conditions. By corona charging experiments a difference in chemical passivation was observed. A higher maximum value of the $S_{\text{eff,max}}(Q_C)$ -plots was found for the Cz substrates as shown in Fig. 3-a. However the initial $S_{\text{eff,max}}$ -values before corona charging were quite similar with $9 \pm 1 \text{ cm/s}$ and $11 \pm 1 \text{ cm/s}$, for Cz and FZ substrates, respectively (Fig. 3-b). By inspection using optical microscopy a significantly rougher surface structure was observed for the Cz substrates as shown in the inset in Fig. 3-a. From the rougher surface morphology and from the higher maximum value of the $S_{\text{eff,max}}(Q_C)$ -plots it can be hypothesized that the chemical passivation was lower for Cz substrates. However the quite similar $S_{\text{eff,max}}$ -values before corona charging experiments revealed that the field-effect passivation mechanism is the dominating passivation mechanism.

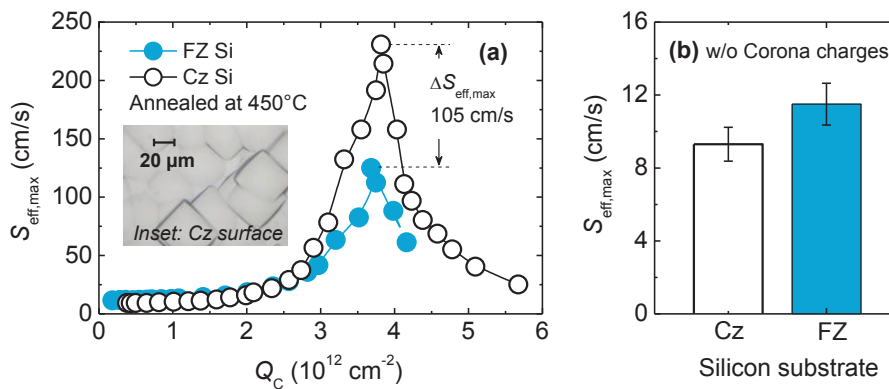


Fig. 3. Effective surface recombination velocity $S_{\text{eff,max}}$ (a) as a function of corona charge density Q_C of ALD Al_2O_3 films grown at 300°C on Cz and FZ n -type Si substrates. The inset in (a) shows an optical microscopy image of a Cz wafer surface. (b) Initial $S_{\text{eff,max}}$ -values obtained for the two types of substrates (before the corona charging procedure)

4. Conclusion

From a study of varying the deposition and anneal temperature of ALD Al_2O_3 films it was found that the surface passivation quality decreases with increasing deposition temperature. Lowest S_{eff} values are achieved for ALD films grown at 200°C . Concerning the variation of annealing temperature an improvement of surface passivation was found with increasing anneal temperature for films grown at 200 and 300°C . That improvement is related to a minor increase in field-effect passivation and a substantial improvement in chemical passivation. In addition it was found that the field-effect passivation mechanism could compensate the lower chemical passivation that was obtained for the passivation of Cz substrates that had a rougher surface than FZ substrates.

Acknowledgements

This work is supported by the German Ministry for Environment, Nature Conservation and Nuclear Safety (BMU) under Contract No. 0325150 (“ALADIN”).

References

- [1] S.W. Glunz, *Advances in OptoElectronics*, 2007; **2007**.
- [2] A. Stesmans and G. Van Gorp, *Appl. Phys. Lett.*, 1990; **57**, 2663.
- [3] H.F.W. Dekkers, L. Carnel, and G. Beaucarne, *Appl. Phys. Lett.*, 2006; **89**, 013508.
- [4] J. Hong et al., *J. Vac. Sci. Technol. B* 2003; **21**, 2123.
- [5] A.G. Aberle, *Crystalline Si solar cells: advanced surface passivation and analysis*, University of New South Wales 1999.
- [6] R. Hezel and K. Jaeger, *J. Electrochem. Soc.* 1989; **136**, 518.
- [7] S. Narasimha and A. Rohatgi, *Appl. Phys. Lett.* 1998; **72**, 1872.
- [8] J. Schmidt, M.J. Kerr, and A. Cuevas, *Semicond. Sci. Technol.* 2001; **16**, 164.
- [9] M. Hofmann et al., *Sol. Energy Mater. Sol. Cells* 2009; **93**, 1074.
- [10] Y. Larionova, V. Mertens, N.-P. Harder, and R. Brendel, *Appl. Phys. Lett.* 2010; **96**, 032105.

- [11] G. Dingemans, M.M. Mandoc, S. Bordihn, M.C.M. van de Sanden, and W.M.M. Kessels, *Appl. Phys. Lett.* 2011; **98**, 1.
- [12] A. Stesmans and V. V. Afanas'ev, *Appl. Phys. Lett.* 2002; **80**, 1957.
- [13] G. Dingemans, W. Beyer, M.C.M. van de Sanden, and W.M.M. Kessels, *Appl. Phys. Lett.* 2010; **97**, 152106.
- [14] A. Wolf, S. Mack, C. Brosinsky, M. Hofmann, P. Saint-Cast, and D. Biro, *37th IEEE PVSC, Seattle, USA* 2011.
- [15] G. Dingemans et al., *J. Appl. Phys.* 2011; **110**, 093715.
- [16] G. Dingemans et al., *J. Appl. Phys.* 2009; **106**, 114907.
- [17] J. Schmidt, B. Veith, F. Werner, D. Zielke, R. Brendel, *Proc. of 35th IEEE PVSC, Honolulu, USA* 2010.
- [18] A. Richter, M. Hörteis, J. Benick, S. Henneck, M. Hermle, S.W. Glunz, *Proc. of 35th IEEE PVSC, Honolulu, USA* 2010.
- [19] B. Veith, F. Werner, D. Zielke, R. Brendel, and J. Schmidt, *En. Proc.* 2011; **8**, 307–312.
- [20] G. Agostinelli et al., *Sol. En. Mat. & Solar Cells* 2006; **90**.
- [21] B. Hoex, S.B.S. Heil, E. Langereis, M.C.M. van de Sanden, and W.M.M. Kessels, *Appl. Phys. Lett.* 2006; **89**, 042112.
- [22] S.E. Potts et al., *J. Electrochem. Soc.* 2010; **157**, 7.
- [23] S.E. Potts, G. Dingemans, G. Lachaud, W.M.M. Kessels, *J. Vac. Sci. Technol. A* 2012; **30**, 2.
- [24] G. Dingemans et al., *Phys. Status Solidi RRL* 2010; **4**, 1 10–12.
- [25] A. G. Aberle, *Prog. Photovoltaics: Res. Appl.* 2000; **8**, 473.
- [26] T. Suntola, *Mat. Sci. Report* 1989; **4**, 7.
- [27] S.W. Glunz, D. Biro, S. Rein, and W. Warta, *J. Appl. Phys.* 1999; **1**, 86.